Pre-selecting muon events in the camera server of the ASTRI telescopes for the Cherenkov Telescope Array

Maria Concetta Maccarone [*a], Teresa Mineo [a], Milvia Capalbi [a], Vito Conforti [b], for the ASTRI Collaboration[d] and the CTA Consortium[e], and Martina Coffaro[c]

[a] INAF, IASF-Palermo, Via Ugo La Malfa 153, 90146 Palermo, Italy
[b] INAF, IASF-Bologna, Via Pietro Gobetti 101, 40129 Bologna, Italy
[c] Uni. Palermo, Dip. Fisica, Viale delle Scienze, 90128 Palermo, Italy
[d] http://www.brera.inaf.it/astri
[e] http://www.cta-observatory.org

ABSTRACT

The Cherenkov Telescope Array (CTA) represents the next generation of ground-based observatories for very high energy gamma-ray astronomy. The CTA will consist of two arrays at two different sites, one in the northern and one in the southern hemisphere. The current CTA design foresees, in the southern site, the installation of many tens of imaging atmospheric Cherenkov telescopes of three different classes, namely large, medium and small, so defined in relation to their mirror area; the northern hemisphere array would consist of few tens of the two larger telescope types. The telescopes will be equipped with cameras composed either of photomultipliers or silicon photomultipliers, and with different trigger and read-out electronics. In such a scenario, several different methods will be used for the telescopes' calibration. Nevertheless, the optical throughput of any CTA telescope, independently of its type, can be calibrated analyzing the characteristic image produced by local atmospheric highly energetic muons that induce the emission of Cherenkov light which is imaged as a ring onto the focal plane if their impact point is relatively close to the telescope optical axis. Large sized telescopes would be able to detect useful muon events under stereo coincidence and such stereo muon events will be directly addressed to the central CTA array data acquisition pipeline to be analyzed. For the medium and small sized telescopes, due to their smaller mirror area and large inter-telescope distance, the stereo coincidence rate will tend to zero; nevertheless, muon events will be detected by single telescopes that must therefore be able to identify them as possible useful calibration candidates, even if no stereo coincidence is available. This is the case for the ASTRI telescopes, proposed as pre-production units of the small size array of the CTA, which are able to detect muon events during regular data taking without requiring any dedicated trigger. We present two fast algorithms to efficiently use uncalibrated data to recognize useful muon events within the single ASTRI camera server while keeping the number of proton-induced triggers as low as possible to avoid saturating the readout budget towards the central CTA data analysis pipeline.

Keywords: Image Atmospheric Cherenkov Telescope, CTA, muon rings, calibration, ASTRI, camera server

1. INTRODUCTION

Highly energetic muons penetrating the atmosphere produce Cherenkov light that is imaged as characteristic arcs or rings by Imaging Atmospheric Cherenkov Telescopes (IACT), if their impact point is relatively close to the telescope optical axis. The analysis of such rings[1] has been recognized as a powerful and precise method to calibrate the optical throughput of any existing IACT system.

The Cherenkov Telescope Array (CTA)[2] foresees three main classes of IACT (large, medium, small) equipped with cameras composed either of photomultipliers or silicon photomultipliers, and with different trigger and read-out electronics. Due to such a variety of telescope systems, differences in muon detection efficiency will be present. A

[*] Cettina.Maccarone@iasf-palermo.inaf.it, http://www.iasf-palermo.inaf.it/~maccarone/

dedicated study was made by the CTA Calibration team to establish the feasibility of detecting and using muon ring images as calibrators[3], with particular attention being paid to the small sized telescopes (SST), present for the first time in the current panorama of the IACT systems. The study confirmed that a muon calibration scheme is viable for all CTA telescopes[4], using regular data taken close to or contemporary with normal science observations, but improving the technique currently applied. It is important to note that large sized telescopes will be able to detect muon images even under a stereo trigger, and such stereo muon events will be passed directly to the central CTA array data acquisition pipeline to be analyzed. For the MST and particularly for the SST telescopes the stereo muon rate will tend to zero, given their smaller mirror area and larger inter-telescope distance, thus degrading the reconstruction power. Dedicated runs with adapted trigger thresholds would then be necessary for the MST and SST telescopes, or sufficiently efficient flagging of muon rings which have triggered only one telescope, so they are not rejected by the stereo coincidence trigger. The latter is the case for the ASTRI telescopes, which will be able to detect single-muon events during regular science data taking without requiring any dedicated trigger.

After a brief description of the ASTRI telescopes, we present two high-speed procedures (based on statistical and morphological approach, respectively) proposed to recognize, at level of the ASTRI camera server, useful single-muon images while rejecting, as much as possible, images produced by proton induced triggers. Both algorithms, designed to operate on-line during regular science data taking, require a preliminary cleaning phase to extract the raw data signal (muon, proton, etc.) from the night sky background in which it is embedded. The statistical algorithm is essentially based on the evaluation of the average count per pixel and on the number of pixels surviving after the cleaning. The morphological algorithm is based on the application of the Taubin method[5] which enables the rapid determination of the geometrical parameters of the circle fitting the ring. The algorithms have been tested on simulated data; their application to real data will come soon. Whatever will be the final choice of the algorithm implemented in the ASTRI camera server, the events flagged as possible single-muon ring images will be analyzed in detail off-line[6] and the outcome will be used for the calibration of the optical throughput, monitoring of the optical point spread function, flat-fielding of the camera, and to evaluate the uniformity of the mirror reflectivity of each ASTRI telescope.

2. THE ASTRI TELESCOPES

Since 2011, the Italian National Institute for Astrophysics (INAF) has been leading the "Astrofisica con Specchi a Tecnologia Replicante Italiana" (ASTRI) project of the Italian Ministry of Education, University and Research. This project aims at designing and developing an end-to-end prototype for the CTA Small Size class of Telescopes (SST) in a dual-mirror configuration (2M)[7]. The prototype telescope, named ASTRI SST-2M and installed in Italy at the INAF "M.C. Fracastoro" observing station located in Serra La Nave (Mt. Etna, Sicily)[8], was inaugurated in September 2014; its completion, with the installation of the camera at the focal plane, is foreseen in the second half of 2016. The calibration and science verification phase will follow with the purpose of assessing the instrument performance by means of observations targeted at bright TeV sources. At the same time, a collaborative and international effort within the CTA framework is being carried on by Italy, Brazil and South-Africa with the aim of deploying, on the CTA southern site, an array of at least nine ASTRI telescopes with a relative distance of the order of 300 m. The ASTRI mini-array, proposed to be part of the CTA pre-production phase, should allow early scientific investigations of prominent sources in the energy range from a few TeV up to hundreds of TeV[9,10].

The ASTRI telescopes are characterized by several innovative technological solutions: the optical system[11] is based on a dual-mirror Schwarzschild-Couder design with a curved focal plane covered by Silicon photomultipliers (SiPMs) sensors managed by a fast front-end electronics[12,13]. The 4.3m diameter primary mirror of the ASTRI SST-2M prototype is composed of an array of hexagonal tiles, while the 1.8m diameter secondary mirror is monolithic; the system covers a 9.6° full field-of-view (FoV). The camera is formed of a matrix of SiPM sensors organized in 37 Photon Detection Modules (PDM) of 8×8 pixels each of them with a sky-projected angular size of 0.17° so matching the angular resolution of the optical system. This configuration yields a Point Spread Function (PSF), defined as the 80% of the light collected from a point like source, contained in one pixel. Some improvements are foreseen with the new generation of SiPM sensors that will be used in the camera of the ASTRI telescopes that will form the mini-array (the FoV could reach a value of 11.2° and the pixel angular size could be enlarged to 0.19°). In both the cases, prototype and mini-array, the front end electronics of the ASTRI camera includes the Cherenkov Imaging Telescope Integrated Read Out Chip (CITIROC) that, with its signal shaper and peak detector customized for ASTRI, provides high efficiency auto-trigger capability and very fast camera pixel read out[14]. The ASTRI camera trigger is a topological one, activated when a given number of contiguous pixels within a PDM presents a signal above a given photo-electron threshold. Both the number of

contiguous pixels required for a trigger and the signal threshold are programmable, depending on the level of Night Sky Background (NSB).

Data registered by the ASTRI camera at the occurrence of a trigger condition (scientific raw event) or when required (calibration, variance and housekeeping data) are then sent to the camera server in which the camera Data AcQuisition software (camera DAQ) is installed[15,16]. In the case of the ASTRI SST-2M prototype, operating in as a single telescope, the camera DAQ software is aimed at the acquisition, pre-processing, storage and monitoring of the camera data; it includes a Quick Look display and interacts with the data handling subsystem in order to transfer the files, after proper format conversion, to the data archive and analysis components[17,18]. In the case of the ASTRI mini-array, the camera server has to interface with the CTA array control and data acquisition system[19]; in such a configuration the camera servers (one for each telescope), in addition to acquiring data without loss, also have to manage the event time stamping and forward the data, applying the stereo trigger selection for the science events, to the central CTA array data acquisition pipeline. The design of the camera server software for the ASTRI telescopes in the mini-array configuration is described elsewhere in these proceedings[20].

3. SELECTING MUON RING IMAGES IN THE ASTRI CAMERA

A description of the relations between cosmic muons and Cherenkov light and of the method by which muons can be used in the calibration of IACT telescopes[1] is outside the scope of this contribution. Nevertheless, it can be useful to recall that when a muon is detected by a IACT telescope, the Cherenkov light emitted in a narrow cone along the final part of its path is imaged as a ring or arc in the camera, depending on the muon impact point onto the optical system. The position of the center of the ring depends on the muon arrival direction with respect to the telescope optical axis. The radius of the ring corresponds to the aperture of the cone (Cherenkov angle), reaching values of around 1.3°, while the muon impact point determines the modulation of light along the ring. The analysis of high-quality ring annular pattern (often called 'good muon rings') allows the reconstruction of the muon physical parameters and the eventual extraction the information useful for the calibration, such as the telescope's optical throughput.

As described elsewhere in these proceedings[6], the ASTRI telescopes are able to provide sufficient high-quality single-muon images per night for accurate calibration. Figure 1 shows an example of simulated muon images, as expected to be seen by the ASTRI camera, embedded in a level of NSB corresponding to an extra-galactic dark sky, without bright stars in the telescope field-of-view; under the set-up configuration used in the present contribution, such a level is equivalent to one photo-electron per pixel (NSB rate about 20 MHz) over the ASTRI camera integration time of the signal (set here at 50 ns). The topological trigger configuration, identical to that used for the regular data taking, is of 5 contiguous pixels inside a PDM, each pixel having a signal above a threshold of 4 photo-electrons.

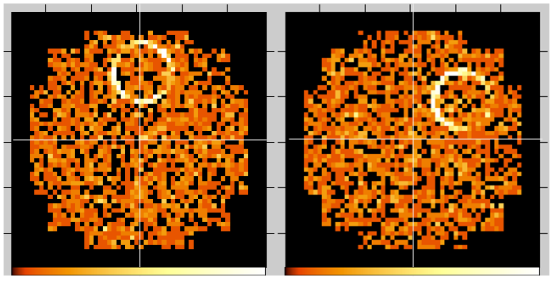

Figure 1. Simulated Cherenkov images of a 40 GeV muon, embedded in the dark night sky background (see text), hitting the primary mirror of ASTRI SST-2M at 1.1 m (left) and at 1.7 m (right) from the center of the telescope, respectively.

The problem that we are facing here concerns the ability to select possible 'good muons' from the rest of events at level of the ASTRI camera server, to which raw data registered by the ASTRI camera are sent. In this section we will describe the two selection methods studied; since they should be applied on-line, both methods are fast, with low requirements on computing power and are optimized to work on raw data.

Moreover, both methods need to be applied on images cleaned of the NSB contribution. The cleaning must maintain the basic shape of the signal and avoid as much as possible the presence of isolated pixels (outliers). A very suitable and fast method is based on a two-level cut algorithm applied to each image pixel with respect to its neighbors within a 3×3 pixels window: pixels with a signal above a given χ_1 threshold are only accepted if they have at least an adjacent pixel

with signal above a certain χ_2 threshold, and vice-versa. The value of the thresholds depends on the level of the NSB; in the case of our simulated data set, we used:

$$\chi_1 = \overline{NSB} + k_1 \cdot RMS(NSB)$$

$$\chi_2 = \overline{NSB} + k_2 \cdot RMS(NSB)$$

where the NSB values (mean and root mean square, *RMS*) can be evaluated from the image by looking at a region where the main significant signal is not present; work is in progress to define a fast and efficient method of achieving this (not presented in this contribution). As a first step, in the procedures described here the NSB is evaluated considering the image as formed only by NSB signal characterized by a Poisson distribution; the contribution of NSB per pixel will then be equal to the mean value $\overline{NSB}$ of the distribution whose standard deviation is $RMS(NSB) = \sqrt{\overline{NSB}}$.

Figure 2 shows some examples, drawn from our simulated data set, of muon and proton-induced trigger images before and after the application of the two-level cut cleaning algorithm.

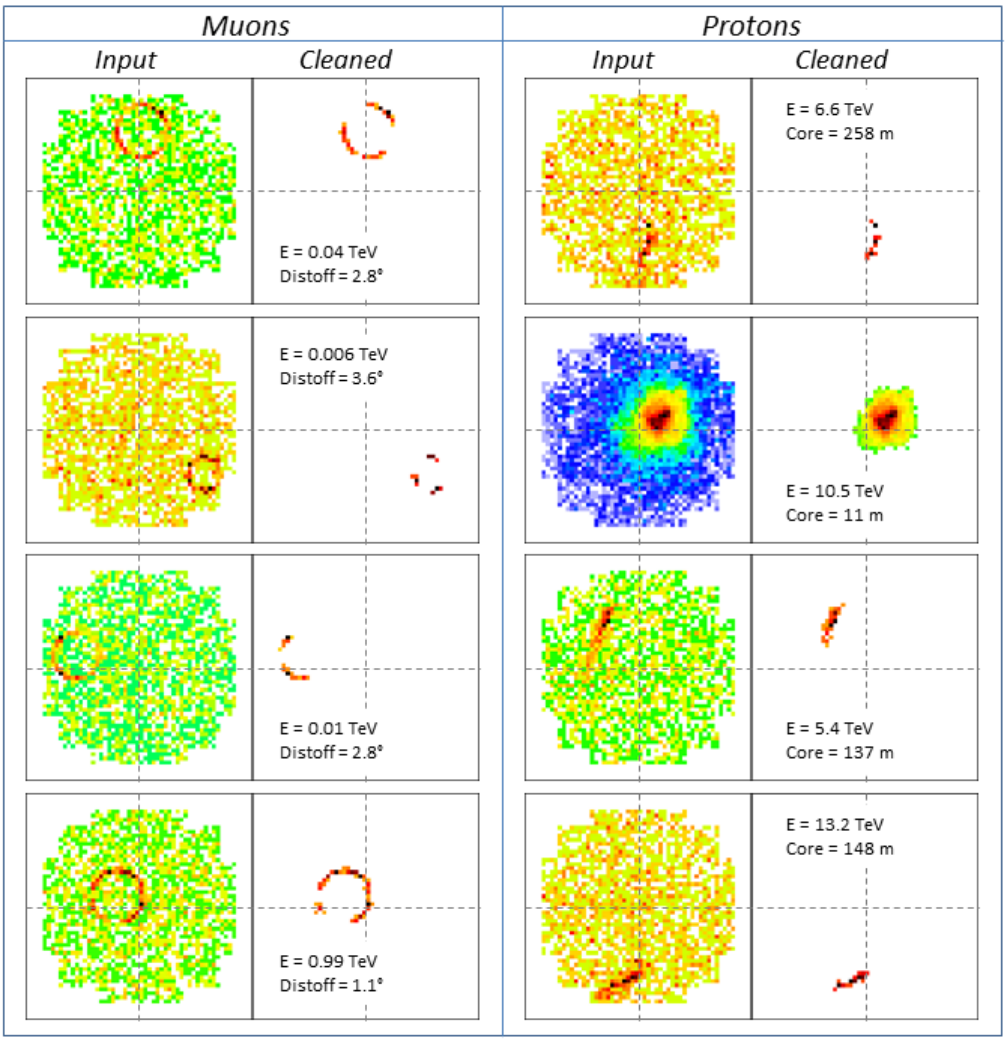

Figure 2. Example of muon and proton events simulated at different primary energies and imaged in the ASTRI camera (Input). For the muon events the angular distance (Distoff) between the muon arrival direction and the telescope optics axis is shown; for the proton events, the distance of the core with respect to the center of the telescope is shown. To clean images from the NSB, the two-level cuts algorithm has been here applied with k_1 and k_2 set to 2 and 5, respectively.

3.1 Statistical approach

The statistical method is based on the expected distributions (a training set from simulated data) of the number of pixels and the average of counts per pixel left after cleaning both for muon and proton events. From such distributions acceptance ranges are identified taking into account that the probability the event has to be a muon must be higher than the probability that it is a proton: that is, the acceptance range is the region of the average of counts per pixel where the distribution is higher for muons than for protons; similarly for the number of pixels left. Each event is flagged as a possible muon candidate depending on the values that these parameters (number of pixels and average of counts per pixel) will assume.

3.2 Morphological approach (Taubin method)

The peculiarity of muon events to be visualized as circular rings, closed or open, has led us to develop a different selection procedure employing a morphological approach. The shape parameters of the circle which best fits a muon ring can be easily determined by applying the Taubin method that allows to "fit implicit curves and surfaces to data minimizing the approximate mean square distance, which is a nonlinear least squares problem. It is independent of the choice of coordinate system, which is a very desirable property for object recognition, position estimation and the stereo matching problem"[5]. The method is purely geometrical, working on the geometric centroid and not on the center of mass. The initial cleaning is therefore necessary not only to make the raw data signal visible out of the noise from NSB but, eventually, to make feasible the application of this geometrical method.

To evaluate the muon ring geometrical parameters, the coordinate of the center (X_C, Y_C) and the radius (R) are computed by minimizing the function ξ defined as:

$$\xi = \frac{\sum_{i=1}^{N_{pix}}[(X_i - X_C)^2 + (Y_i - Y_C)^2 - R^2]^2}{\sum_{i=1}^{N_{pix}}[(X_i - X_C)^2 + (Y_i - Y_C)^2]}$$

where X_i and Y_i are the image coordinates of the N_{pix} pixels surviving the image cleaning. Due to the cleaning, N_{pix} is typically orders of magnitude smaller than the number of photo-sensors in the camera. The fit is computationally reasonable and few N_{pix} (points) are sufficient to obtain a goodness-of-fit suitable for our purposes. Moreover, only a few iterations are needed to minimize the function in the case of a circle, so that the fit is easily computed in real time.

The aim of the pre-selection at level of the ASTRI camera server is twofold: recognize the largest number of muons from the rest of events registered by the ASTRI camera and identify them as possible candidates to produce 'good muon ring' images fully contained in the camera. To meet this requirement, the main selection criteria to be satisfied concern the success of the Taubin fit and the values of the reconstructed Taubin parameters:

- the Taubin fit must be satisfied in few iterations;
- the ring images with small reconstructed Taubin radius, i.e. small Cherenkov angle, must be rejected since they can be affected by secondary ring-broadening effects that could hamper the accuracy of the calibration;
- a maximum distance between the ring center and camera center has to be defined to exclude muons inclined at large angles that are imaged at the camera edges, where they are often affected by inefficiencies and aberration.

Additional criteria to select 'good muon rings' can be applied to geometrical quantities derived from the Taubin parameters, among them the ratio between the width of the ring and the radius of the circle; this last condition enables empty circles to be distinguished from full circular shapes. Very importantly, this selection procedure is un-biased, especially with respect to the retrieved optical throughput of the telescope.

4. SIMULATION AND RESULTS

The two algorithms have been applied on a mixed data set of muon and proton events, simulated starting from the telescope configuration of the ASTRI SST-2M prototype, and applying the geographical coordinates and atmospheric conditions for the CTA southern site where it is proposed to install the mini-array of at least nine ASTRI telescopes.

Two million μ^+ and μ^- events and one million proton events have been simulated with CORSIKA[21] (version 6.99, IACT/ATMEXT 1.47). The observations take place at 2150m under a quasi-tropical atmosphere[22]. The ASTRI SST-2M telescope is pointing to the zenith and, to cover its full field of view, the events are randomly distributed over a viewing

cone of 4° around the vertical axis. Muon energies are randomized, in the range from 6 GeV to 1 TeV, using a power-law with spectral index 2 (this value was chosen in order to save simulation time during the first phase of our study[3]). The injection height, i.e. the muon starting altitude, has been defined at about 753 g/cm^2, corresponding to 500 m above the observation level. The muon impact parameter ranges within the radius of the ASTRI SST-2M primary mirror (2.1m). Proton energies are randomized using a power-law with spectral index 2.7, in the range 2-100 TeV; protons are randomly distributed with core distances within 400m of the center of the telescope.

The simulation of the ASTRI SST-2M telescope has been performed by using a specific code[23] developed by the ASTRI Collaboration; it is a stand-alone ray-tracing code that checks for the interactions of the input photons with all telescope components and follows them up to the eventual detection in the camera at the focal plane. The code allows for the addition of different levels of NSB. The basic NSB rate applied here corresponds to the extra-galactic dark sky without bright stars in the FoV of the telescope, i.e. one photo-electron per camera pixel in 50 ns, which corresponds to the ASTRI camera integration time (NSB rate: 20 MHz per pixel).

The ASTRI camera trigger has been simulated inside our private codes (IDL and FORTRAN-77) where selection algorithms are currently implemented for test purposes. The topological trigger configuration is of 5 contiguous pixels inside a PDM, each pixel with signal above a threshold of 4 photo-electrons; such a configuration, identical to that foreseen for all events during the regular data taking under the given NSB rate, enables the camera to trigger on almost all (about 99%) of our simulated muon events.

To clean the images, the two-level cut algorithm has been applied with thresholds k_1 and k_2 set to 2 and 5, respectively. Such cuts allow the core shape of the signal to be maintained while avoiding the presence of isolated pixels (outliers); moreover, the cleaned images (see example in Fig.2) contain sufficient pixels above threshold to apply the Taubin fit method ($N_{pix} \geq 5$), avoiding loss of potentially useful muon images.

4.1 Statistical selection and results

The statistical selection has been applied using both a single and two-level cut cleaning. The simpler cleaning, based on a single threshold χ_1 , has been applied with increasing values of k_1 of 5, 7 and 10. The values for the two-level cut cleaning are the same adopted for the morphological selection method (k_1 =2, k_2 = 5).

The statistical algorithm yields similar results for both the number of pixels and the average of counts per pixel left after cleaning; moreover, whatever the cleaning adopted (single or two-level cut) or the values of parameters, the results do not shown any substantial difference: the selection power for muons leaves between 90% and 95% of events, discarding only between 60% and 70% of protons.

4.2 Morphological selection (Taubin' method) and results

The first selection is obtained requiring that the Taubin fit be satisfied in less than 10 iterations ($N_{iter} < 10$); with respect to the total number of triggered events, the resulting percentage of remaining images is ~99% muons and ~56% protons.

The next selection criteria concern the geometry of the fitted circle. The first of them has the purpose of selecting rings fully contained in the camera, avoiding rings with a radius R that is too small and within a maximum distance (*CenterDistance*) between the ring center and camera center. Taking into account the ASTRI SST-2M size, this criterion corresponds to satisfying the following condition:

$$0.5° \leq R \leq 1.5° \quad .and. \quad CenterDistance < 4.5°$$

Figure 3 shows the distribution of these two parameters in our simulation data set selected for $N_{iter} < 10$. The distribution of the radius R (left panel) clearly shows that a consistent fraction of proton images has been fitted by a Taubin circle that is too narrow or too wide. Moreover, the majority of the circles reconstructed from the proton images have their centers very far from the center of the camera (right panel). By applying the selection criterion related to R and *CenterDistance*, (dotted boxes in Fig.3), the resulting percentage of remaining images is 97% muons and 16% protons. It is worthwhile noting that adopting more stringent upper limits could improve the resulting percentages, mainly with regard to the remaining protons; nevertheless, in this study based on simulated data, we preferred to maintain a certain level of contingency and more appropriate limits will be considered in a future, when the entire procedure will be tested on real data.

A further selection can be applied to distinguish empty from full Taubin circles. This can be performed by monitoring the parameter here called *Fullness*, defined as the ratio between the root mean square of the Taubin reconstructed radius, *RMS(R)*, and the radius itself:

$$Fullness = \frac{RMS(R)}{R}$$

The *Fullness* tends to 0 for empty circular shape. Figure 4 shows the distribution of the *Fullness* in our simulation data set selected for $N_{iter} < 10$. To be consistent with the previous selection criteria, we have also adopted a conservative limit value in this case: adding the condition *Fullness* < 0.2°, (dotted box in Fig.4), the percentage of remaining images is about 96% muons and 8% protons.

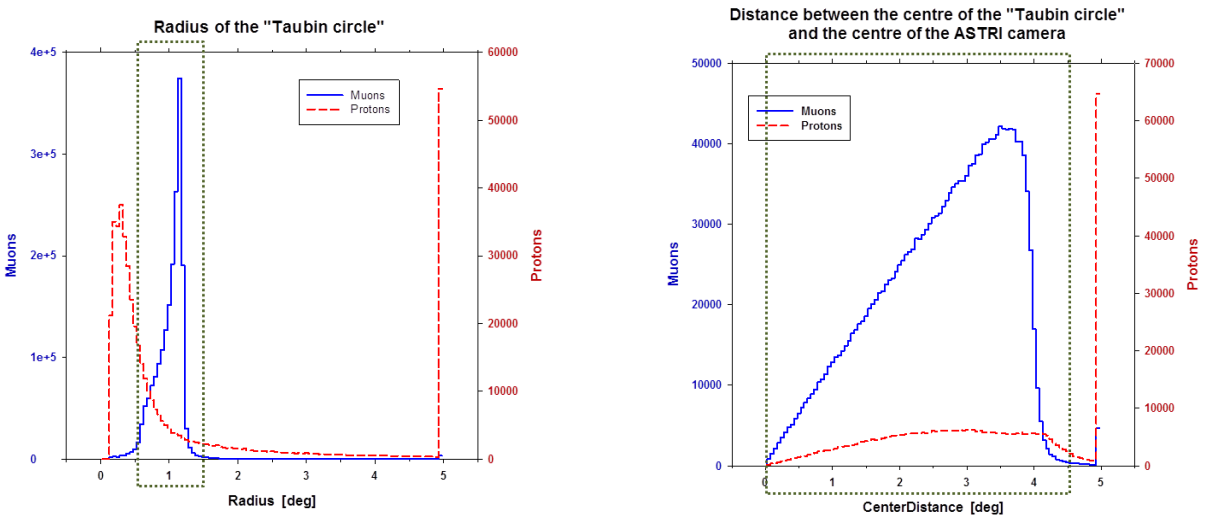

Figure 3. Morphological selection (Taubin method). Distribution of the reconstructed ring parameters *R* (left panel) and *CenterDistance* (right panel) of the images surviving to the first selection (goodness of the Taubin fit). The dotted boxes in both the graphs indicate the limits chosen to be applied for the next selection. The 'exaggerated' number of protons at *R=5 deg* and *CenterDistance=5 deg* is simply an artifact after dumping the overflow into these bins.

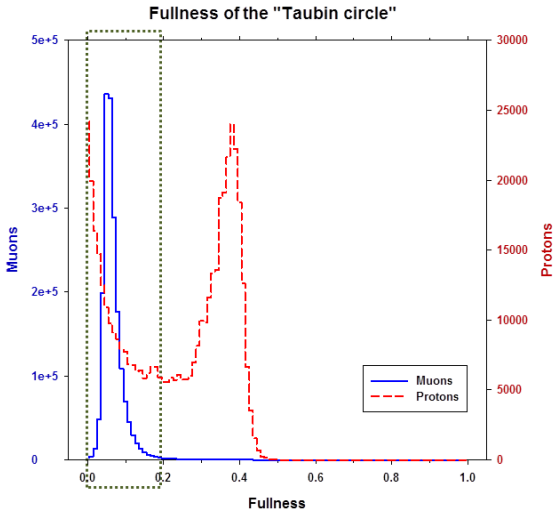

Figure 4. Morphological selection (Taubin method). Distribution of the *Fullness* of the images surviving to the first selection (goodness of the Taubin fit). The dotted box indicates the limits to be used to complete the selection.

5. DISCUSSION AND CONCLUSIONS

The analysis of ring images produced by highly energetic muon events is a powerful method of calibrating the optical throughput of any IACT. In the CTA context, large and medium telescopes are able to detect muon events useful for calibration even under the stereo requirement, and such stereo muon events will be sent directly to the central CTA array data acquisition pipeline to be analyzed. This is not feasible for the ASTRI telescopes because the stereo muon rate will be nearly zero, given the ASTRI's small mirror area and large inter-telescope distance. Therefore, if we want to use muons as calibrators, we have to act at level of each single telescope and flag those events in some way before sending them to the central analysis pipeline. Muon events are triggered by the ASTRI camera during the regular science data taking under the same topological trigger configuration used for gamma and protons (5 contiguous pixels inside a PDM, each pixel with signal above a threshold of 4 photo-electrons); in terms of data rate, a total of 4 muons per second impacting onto the ASTRI primary mirror[6] is expected to be triggered while the proton-induced trigger rate[24] is of the order of 150 per second. Such muon events are sent to the ASTRI camera server, which has to perform several acquisition and data management functions. Our aim is therefore to define a proper pre-selection algorithm to be implemented at level of the ASTRI camera server without jeopardizing its performance. The algorithm, designed to be operated on-line, must be fast, computationally efficient and, at the same time, it must keep the number of unhelpful or misleading events as low as possible to avoid saturating the readout budget of the central CTA pipeline.

Both the procedures proposed in this contribution, whose results are summarized in Table 1, seem to satisfy all the constraints, although with some differences.

The statistical method is the simplest one. The average count per pixel and the number of pixels surviving in the image cleaned of the NSB are taken into account, resulting in an average selection efficiency of the order of 93% for muons and 35% for protons. Such results, although satisfactory from the muon selection point of view, retain a large number of proton-induced triggers that could saturate readout in the future CTA data acquisition system.

The morphological method is more efficient and, with the selection criteria applied, the resulting efficiency is of the order of 96% for muons while keeping the number of proton-induced triggers of the order of 8%.

It is worth noting that the resulting percentages and data rate values could improve if more stringent upper limits on the selection criteria are adopted; this will be considered in the future, when the entire procedure will be tested on real data.

Table 1. Percentage of surviving events w.r.t. triggered events after cleaning and the application of the statistical and morphological selection methods. The variability in the statistical approach depends on the parameter of interest for the selection (number of pixels or average of the counts left after cleaning, respectively).

Event	**Percentage of events selected as possible muon candidate**	
	Statistical approach	**Morphological approach**
Protons	30-40 %	8 %
Muons	90-95 %	96 %

It has to be noted that both the methods will be applied on uncalibrated images (as coming from the camera) and require a preliminary cleaning phase to make the raw data signal (muon, proton, etc.) visible out of the night sky background in which it is embedded. Improvements in the selection efficiency can be foreseen by defining a more detailed evaluation of the NSB from each image. A study of this, together with the dependence of the cleaning cut values w.r.t. different NSB levels, is in progress.

It is worthwhile mentioning that the parameters and values adopted in the pre-selection phase must be directed to recognize in real time the largest number of possible candidate muons from the rest of triggered events without needing to go into the details of a deep analysis of the image.

Both algorithms will be tested on real data as acquired with the ASTRI SST-2M prototype and then optimized in view of their implementation in the camera server of the ASTRI telescopes proposed under the CTA configuration. The choice will also depend on the data volume and rate. Whatever the final choice, the events flagged as possible candidates for producing usable single-muon ring images will be analyzed in detail off-line for the calibration of the optical throughput of the telescope.

ACKNOWLEDGMENTS

This work is supported by the Italian Ministry of Education, University, and Research (MIUR) with funds specifically assigned to the Italian National Institute of Astrophysics (INAF) for the Cherenkov Telescope Array (CTA), and by the Italian Ministry of Economic Development (MISE) within the "Astronomia Industriale" program. We acknowledge support from the Brazilian Funding Agency FAPESP (Grant 2013/10559-5) and from the South African Department of Science and Technology through Funding Agreement 0227/2014 for the South African Gamma-Ray Astronomy Programme. We gratefully acknowledge support from the agencies and organizations listed under Funding Agencies at this website: http://www.cta-observatory.org/.

This paper has gone through internal review by the CTA Consortium.

REFERENCES

[1] Vacanti, G., Fleury, P., Jiang, Y., Paré, E., Rovero, A. C., Sarazin, X., Urban, M., Weekes, T. C.,. "Muon ring images with an atmospheric Cherenkov telescope", Astroparticle Physics 2, 1-11 (1994).

[2] Acharya, B. S., et al., The CTA Consortium, "Introducing the CTA concept", Astroparticle Physics 43, 3-18 (2013).

[3] Gaug, M., Armstrong, T. Bernlohr, K., Daniel, M., Errando, M., Maccarone. M.C., Majumdar, P., Mineo, T., Mitchell, A., Moderski, R., Parsons, D., Prandini, E., Toscano, S., "Using Muon Rings for the Optical Throughput Calibration of the Cherenkov Telescope Array", CTA COM-CCF/150310, v.4.7 (2015).

[4] Gaug, M., Berge, D., Daniel, M., Doro, M., Förster, A., Hofmann, W., Maccarone, M.C., Parsons, D., Van Eldik, Ch., for the CTA Consortium, "Calibration strategy of the Cherenkov Telescope Array", Proc. SPIE 9149, Observatory Operations: Strategies, Processes, and Systems V, 914919; doi:10.1117/12.2054536 (2014).

[5] Taubin, G., " Estimation of planar curves, surfaces, and nonplanar space curves defined by implicit equations with applications to edge and range image segmentation". IEEE Trans. Pattern Anal. Mach. Intell. 13 (11), 1115-1138 (1991).

[6] Mineo, T., Maccarone, M.C, et al., "Using muon rings for the optical calibration of the ASTRI telescopes for the Cherenkov Telescope Array", *these proceedings* (2016).

[7] Pareschi, G, et al, for the CTA Consortium, "The dual-mirror Small Size Telescope for the Cherenkov Telescope Array", Proc.33rd ICRC, arXiv:1307.4962 (2013).

[8] Maccarone, M.C., Leto, G., et al, for the ASTRI Collaboration, "The Site of the ASTRI SST-2M Telescope Prototype", Proc.33rd ICRC, arXiv:1307.5139 (2013).

[9] Vercellone, S., for the ASTRI Collaboration and the CTA Consortium, "The ASTRI mini-array within the Cherenkov Telescope Array", Proc. RICAP 2014, EPJ-EDP Sciences, arXiv: 1508.00799, (2015).

[10] Pareschi, G., Bonnoli, G., Vercellone, S., on behalf of the ASTRI Collaboration and for the CTA Consortium, "The mini-array of ASTRI SST-2M telescopes, precursors for the Cherenkov Telescope Array", Procs. 14th TAUP 2015, (2016).

[11] Canestrari, R, Cascone, E., et al, for the ASTRI Collaboration, "The ASTRI SST-2M Prototype: Structure and Mirror", Proc. 33rd ICRC, arXiv:1307.4851 (2013).

[12] Catalano, O., Maccarone, M.C., et al, for the ASTRI Collaboration and the CTA Consortium, "The camera of the ASTRI SST-2M prototype for the Cherenkov Telescope Array", Proc. SPIE 9147, doi: 10.1117/12.2055099, (2014).

[13] Sottile, G., Catalano, O., et al, for the ASTRI Collaboration and the CTA Consortium, "ASTRI Camera Electronics", *these proceedings* (2016).

[14] Impiombato, D., Giarrusso, S., et al, "Characterization and performance of the ASIC (CITIROC) front-end of the ASTRI camera", Nucl. Instr. and Methods in Physics Research A, 794,185 (2015)

[15] Conforti, V., Trifoglio, et al, for the ASTRI Collaboration and the CTA Consortium, "The ASTRI SST-2M telescope prototype for the Cherenkov Telescope Array: camera DAQ software architecture", Proc. SPIE 9152, doi:10.1117/12.2054519 (2014).

[16] Conforti, V., Trifoglio, et al, for the ASTRI Collaboration and the CTA Consortium, "The Camera Server of the ASTRI SST-2M Telescopes proposed for the Cherenkov Telescope Array", Proc. 25th ADASS (2015).

[17] Tosti, G., Schwarz, et al, , for the ASTRI Collaboration and the CTA Consortium, "The ASTRI MASS Software System", Proc. SPIE 9152, doi: 10.1117/12.2055067, (2014).

[18] Antonelli, L.A., Bastieri, D., et al, for the ASTRI Collaboration and the CTA Consortium, "The ASTRI Project within Cherenkov Telescope Array: data analysis and archiving", Proc. SPIE 9147, doi: 10.1117/12.2055099, (2014).
[19] Oya, I., Fuessling, M., et al, for the CTA Consortium, "Status and Plans for the Array Control and Data Acquisition System of the Cherenkov Telescope Array", Proc. 34th ICRC, arXiv:1509.01164 (2015).
[20] Conforti, V., Trifoglio, M., et al, for the ASTRI Collaboration and the CTA Consortium, "Software design of the ASTRI Camera Server proposed for the Cherenkov Telescope Array", *these proceedings* (2016).
[21] Heck, D., Knapp, J., Capdevielle, J.N., Schatz, G., and Thouw, T., "CORSIKA: A Monte Carlo code to simulate Extensive Air Showers", Forschungs-zentrum Karlsruhe Report FZKA 6019 (1998).
[22] Bernlöhr, K., private communication (2015)
[23] Cusumano, G., La Parola, V., Mineo, "Basic simulator for the ASTRI SST-2M single prototype." ASTRI-TN-IASFPA-3300-008 Technical Report (2013)
[24] Cusumano, G., La Parola, V., Mineo, "Trigger simulator for the ASTRI SST-2M telescope." ASTRI-TN-IASFPA-3300-024 Technical Report (2015)